Inorg. Chem. **2006**, *45*, 7642–7650

Assembling of Dimeric Entities of Cd(II) with 6-Mercaptopurine to Afford One-Dimensional Coordination Polymers: Synthesis and Scanning Probe Microscopy Characterization

Pilar Amo-Ochoa,*,‡ M Isabel Rodríguez-Tapiador,‡ Oscar Castillo,*,§ David Olea,|| Alejandro Guijarro,† Simone S. Alexandre,|| Julio Gómez-Herrero,|| and Félix Zamora*,†

Departamento de Tecnología Industrial, Universidad Alfonso X "El Sabio", 28691 Villanueva de la Cañada, Madrid, Spain, Departamento de Química Inorgánica, Facultad de Ciencia y Tecnología, Universidad del País Vasco, Apartado 644, E-48080 Bilbao, Spain, Departamento de Física de la Materia Condensada, Universidad Autónoma de Madrid, 28049 Madrid, Spain, and Departamento de Química Inorgánica, Universidad Autónoma de Madrid, 28049 Madrid, Spain

Received March 8, 2006

The direct reaction between 6-mercaptopurine (6-MP) and Cd^{II} under different conditions yields either $[Cd_2(6\text{-}MP)_4(NO_3)_2](NO_3)_2$ (**1**) or $[Cd(6\text{-}MP^{-})_2{\cdot}2H_2O]_n$ (**4**). Compound **1** behaves as the building block of the polymer $[Cd(6\text{-}MP^{2-})_2]_n[Ca(H_2O)_6]_n$ (**3**), by deprotonation of 6-MP ligand. In the reaction of **1** to give **3**, the dinuclear compound $[Cd_2(6\text{-}MP)_4(H_2O)_2](NO_3)_4{\cdot}2H_2O$ (**2**) can be isolated as an intermediate. Polymers **3** and **4** convert into each other in water via deprotonation–protonation reactions. The structures of compounds **1**–**3** have been determined by X-ray diffraction. Given the small differences in the arrangement shown in the crystal structures of the polymer **4** and the polyanion of **3**, the stabilities and energetics of the two arrangements have been examined by DFT calculations to determine the possibility of identifying new conformations of both polymers. In addition, the two polymers have been characterized on surfaces by means of AFM. The direct reaction between 6-MP and Cd^{II} and the deprotonation of the polymer **4** have proven to be useful routes for the isolation of one-dimensional systems on surfaces. The development of new strategies to characterize these types of polymers on surfaces opens the possibility to perform nanoscale studies on their properties and their potential use as nanomaterials.

Introduction

One-dimensional nanostructures (wires, rods, tubes, tapes, etc.) are materials with at least one dimension between 1 and 100 nm. Because of their potential applications in nanotechnology, these systems have recently received much attention.[1,2] It is obvious that one of the most interesting applications of 1D structures is in nanoelectronics. However, there are also many other feasible nanoapplications, such as mechanical sensors, optical elements, and structures useful for biological systems, among others.[1] Two approaches can be followed to generate nano-components: (i) *top-down* and (ii) biomimetic *bottom-up* strategies. In the first one, some photolithography and microcontact printing processes allow transistors of just 50 nm to be obtained, but these techniques have already reached their limits. In the second one, the self-assembly of molecules produces materials ranging from 5 nm to several micrometers. The self-assembly *bottom-up* processes are used by nature to generate functional nano-systems such as proteins, DNA, ribosomes, etc. Supramolecular chemistry holds together, by noncovalent bonds, suitable building blocks to create larger aggregates. Coordination bonds have been extensively used to create one-, two-, and three-dimensional supramolecules, named as coordination polymers. The suitable selection of the building blocks, metals or complexes and organic fragments, may allow the generation of a wide range of architectures. These types of polymers have recently received much attention

* To whom correspondence should be addressed. E-mail: pamochoa@uax (P.A.); oscar.castillo@ehu.es (O.C.); felix.zamora@uam.es (F.Z.).
‡ Departamento de Tecnología Industrial, Universidad Alfonso X "El Sabio".
§ Departamento de Química Inorgánica, Universidad del País Vasco.
|| Departamento de Física de la Materia Condensada, Universidad Autónoma de Madrid.
† Departamento de Química Inorgánica, Universidad Autónoma de Madrid.

(1) Xia, Y. N.; Yang, P. D.; Sun, Y. G.; Wu, Y. Y.; Mayers, B.; Gates, B.; Yin, Y. D.; Kim, F.; Yan, Y. Q. *Adv. Mater.* **2003**, *15*, 353−389.
(2) Xia, Y. N.; Yang, P. D. *Adv. Mater.* **2003**, *15*, 351−352.

10.1021/ic060384f CCC: $33.50
Published on Web 08/25/2006

becauser of their potential applications in several areas, such as catalysis, electronics, photochemistry, and magnetochemistry.[3,4] However, despite a large number of coordination polymers that have been synthesized, few works have centered on the study of their applications in nanotechnology.[5−7] This fact is probably a consequence of their restricted processability, as a consequence of their lack of solubility, rapid degradation in solution, and decomposition upon heating. In particular, reports on the synthesis and characterization of isolated chains of one-dimensional coordination polymers on surfaces are more limited than those of two-dimensional systems.[6]

Recently, we studied the one-dimensional coordination polymer $[Cd(6\text{-}MP^{-})_2\cdot 2H_2O]_n$ (6-MP = 6-mercaptopurine) to verify its processability as a nanomaterial. Using ultrasound, we have been able to isolate and characterize, on mica, single chains of this polymer by atomic force microscopy (AFM).[8] This work has demonstrated the potential use of coordination polymers as molecular wires. Additionally, in a related work, we have characterized, by AFM and STM, the one-dimensional coordination polymer $[Mn(\mu\text{-ox})(4atr)_2]_n$ (ox = oxalato and 4atr = 4-amine-1,2,4-triazole) on mica and highly oriented pyrolitic graphite (HOPG). We have observed a significant effect of the nature of the surface on the organization of the polymer.[9] The present work deals with the synthesis and X-ray characterization of a new polyanion, derived from the one-dimensional polymer $[Cd(6\text{-}MP^{-})_2\cdot 2H_2O]_n$, and two new dinuclear 6-mercatopurine complexes. Special attention has been paid to the development of different ways to isolate one-dimensional coordination polymers on surfaces.

Experimental Section

Materials. All chemicals were of reagent grade and were used as commercially obtained. Elemental analyses were performed on a LECO CHNS-932 microanalyzer.

Synthesis of $[Cd_2(6\text{-}MP)_4(NO_3)_2](NO_3)_2$ (1). $6\text{-}MP\cdot H_2O$ (0.400 g, 2.35 mmol) was dissolved in methanol (10 mL) and added to a solution of $Cd(NO_3)_2\cdot 4H_2O$ (0.560 g, 1.81 mmol) in the same solvent (10 mL). Then, the mixture was stirred at 60 °C for 24 h, and the yellow solid obtained was filtered off, washed with methanol, and dried in air (0.661 g, 67% yield). When the solution had stood for 10 days at 4 °C, crystals of the same compound were formed (0.020 g, 2.0% yield). Anal. Calcd (found) for $C_{20}H_{16}Cd_2N_{20}O_{12}S_4$: C, 22.21 (22.20); H, 1.49 (1.54); N, 25.90 (26.07); S, 11.86 (12.01). IR selected data (KBr, cm^{-1}): 3551 (m,br), 3129 (s), 2960 (s), 1603 (vs), 1580 (s), 1551 (m), 1471 (m), 1407 (m), 1373 (m), 1330 (m), 1306 (m), 1288 (s), 1210 (m), 1015 (m), 950 (m), 860 (m), 641 (m), 515 (m).^{113}Cd NMR (CP/MAS): δ 233.^{1}H NMR (300 MHz, DMSO-d_6): δ 13.77 (s, 1H, N(9)H), 8.40 (s, 1H, H(2)), 8.21 (s, 1H, H(8)).

Synthesis of $[Cd_2(6\text{-}MP)_4(H_2O)_2](NO_3)_4\cdot 2H_2O$ (2). Compound **1** (0.249 g, 0.23 mmol) was stirred in water (25 mL) for 24 h at 20 °C. The pale yellow solid was filtered off, washed with water, and dried in air (0.114 g, 42.9%). when the solution had stood for 10 days at 4 °C, crystals of compound **2** were formed (0.01 g, 3.8% yield). Anal. Calcd (found) for $C_{20}H_{24}Cd_2N_{20}O_{16}S_4$: C, 20.82 (20.38); H, 2.10 (2.12); N, 24.28 (23.81); S, 11.12 (10.99). IR selected data (KBr, cm^{-1}): 3089 (s), 2819 (s), 2760 (s), 1607 (s), 1578 (s), 1432 (m), 1412 (s), 1384 (s), 1333 (vs), 1216 (s), 948 (m), 860 (m), 648 (m), 600(m). ^{113}Cd NMR (CP/MAS): δ 313.^{1}H NMR (300 MHz, DMSO-d_6): δ 13.80 (s, 1H, N(9)H), 8.40 (s, 1H, H(2)), 8.21 (s, 1H, H(8)).

Synthesis of $[Cd(6\text{-}MP^{2-})_2]_n[Ca(H_2O)_6]_n$ (3). Procedure A. A suspension of compound **1** (0.100 g, 0.10 mmol) in water (6 mL) was treated with 23 mL of a water solution of NaOH (0.1 mol L^{-1}). The mixture was stirred at 20 °C for 30 min. The solution obtained was filtered, and 10 mL of a water solution of $Ca(NO_3)_2\cdot 4H_2O$ 0.1 mol L^{-1} was added. A white solid formed immediately. The suspension was stirred for 15 min and then filtered, washed with water and methanol, and dried in air (0.07 g, 67.5% yield). After the clear solution stood at 20 °C for three weeks, crystals of compound **3** were formed (0.010 g, 9.6% yield).

Procedure B. A suspension of compound **4** (0.100 g, 0.222 mmol) in water (5 mL) was treated with 40 mL of a water solution of NaOH (0.1 mol L^{-1}), and the mixture was stirred at 20 °C for 24 h. Then, the mixture was filtered through a pad of Celite, and 10 mL of a 0.1 mol L^{-1} water solution of $Ca(NO_3)_2\cdot 4H_2O$ was added to the clear solution and stirred. Formation of a white solid is observed within a few minutes. The solid was filtered off, washed with water, and dried in air (0.086 g, 69.1% yield).

Anal. Calcd (found) for $C_{10}H_{16}CaCdN_8O_6S_2$: C, 21.41 (21.19); H, 2.88 (2.60); N, 19.98 (19.64); S, 11.43 (11.33). IR selected data (KBr, cm^{-1}): 3082(w), 2918(w), 1634(w), 1566(s), 1429(w), 1384(s), 1261(m), 1101(m), 1019(m), 877(w), 799(w), 512(w).^{113}Cd NMR (CP/MAS): δ 367.

Synthesis of $[Cd(6\text{-}MP^{-})_2\cdot 2H_2O]_n$ (4). The direct general route to obtain this compound has been previously reported by Gosh and Chatterjee,[10] and more concise conditions have also been described by Dubler and Gry.[11] Herein, we report an alternative way to obtain compound **4**. To a water (50 mL) suspension of compound **3** (0.100 g, 0.178 mmol), a solution of HNO_3 (4.8 mol L^{-1}) was added to adjust the pH to ca. 4.0. Then the mixture was stirring at 20 °C for 24 h, after that, the yellow solid obtained was filtered off, washed with water and ethanol, and dried in air (0.051 g, 63.4% yield). Anal. Calcd (found) for $C_{10}H_{10}CdN_8O_2S_2$: C, 26.65 (26.66); H, 2.24 (2.25); N, 24.86 (25.00); S, 14.22 (13.98). IR selected data (KBr, cm^{-1}): 3089 (s), 2819 (s), 2760 (s), 1607 (s), 1578 (s), 1432 (m), 1412 (s), 1384 (s), 1333 (vs), 1216 (s), 948 (m), 860 (m), 648 (m), 600(m). ^{113}Cd NMR (CP/MAS): δ 313.^{1}H NMR (300 MHz, DMSO-d_6): δ 13.80 (s, 1H, N(9)H), 8.40 (s, 1H, H(2)), 8.21 (s, 1H, H(8)).

Preparation of the Surfaces. To obtain reproducible results, very flat surfaces with precisely controlled chemical functionalities, freshly prepared just before the chemical deposition, were used.

(3) Janiak, C. *Dalton Trans.* **2003**, 2781−2804.
(4) Kitagawa, S.; Noro, S. In *Comprehensive Coordination Chemistry II*; Elsevier: Amsterdam, 2004; Vol. 7.
(5) Stepanow, S.; Lingenfelder, M.; Dmitriev, A.; Spillmann, H.; Delvigne, E.; Lin, N.; Deng, X. B.; Cai, C. Z.; Barth, J. V.; Kern, K. *Nature Mater.* **2004**, *3*, 229−233.
(6) Novokmet, S.; Alam, M. S.; Dremov, V.; Heinemann, F. W.; Muller, P.; Alsfasser, R. *Angew. Chem., Int. Ed.* **2005**, *44*, 803−806.
(7) Kurth, D. G.; Severin, N.; Rabe, J. P. *Angew. Chem., Int. Ed.* **2002**, *41*, 3681−3683.
(8) Olea, D.; Alexandre, S. S.; Amo-Ochoa, P.; Guijarro, A.; de Jesús, F.; Soler, J. M.; de Pablo, P. J.; Zamora, F.; Gómez-Herrero, J. *Adv. Mater.* **2005**, *17*, 1761−1765.
(9) Garcia-Couceiro, U.; Olea, D.; Castillo, O.; Luque, A.; Roman, P.; de Pablo, P. J.; Gomez-Herrero, J.; Zamora, F. *Inorg. Chem.* **2005**, *44*, 8343−8348.
(10) Gosh, A. K.; Chatterjee, S. *J. Inorg. Nucl. Chem.* **1964**, *26*, 1459−1461.
(11) Dubler, E.; Gyr, E. *Inorg. Chem.* **1988**, *27*, 1466−1473.

Table 1. Single-Crystal Data and Structure Refinement Details

	1	2	3
formula	$C_{20}H_{16}Cd_2N_{20}O_{12}S_4$	$C_{20}H_{24}Cd_2N_{20}O_{16}S_4$	$C_{10}H_{16}CaCdN_8O_6S_2$
w (g mol^{-1})	1081.63	1153.64	560.91
λ (Å)	1.54178	0.71069	0.71069
T (K)	100(2)	293(2)	293(2)
space group	$P2_1/n$	$P\bar{1}$	$C2/c$
a (Å)	7.1777(1)	7.294(2)	13.864(2)
b (Å)	10.3363(1)	10.730(3)	16.701(2)
c (Å)	22.9074(3)	12.796(3)	8.278(1)
α (deg)	90(−)	110.08(2)	90(−)
β (deg)	94.024(1)	95.45(2)	104.27(1)
γ (deg)	90(−)	96.82(2)	90(−)
V (Å^3)	1695.33(4)	924.0(4)	1857.6(4)
Z	2	1	4
μ (mm^{-1})	13.189	1.477	1.725
D_{calcd} (Mg m^{-3})	2.119	2.073	2.006
reflns collected	10 585	6724	8008
independent reflns	3111	3950	2729
reflns [$I > 2\sigma(I)$]	2873	1641	1666
params	294	235	153
$\Delta\rho_{max,min}$ (e Å^{-3})	0.48, −0.31	0.96, −0.40	0.82, −0.35
final R[a] indexes	R1 = 0.0243	R1 = 0.0606	R1 = 0.0289
[$I > 2\sigma(I)$]	wR2 = 0.0624	wR2 = 0.1344	wR2 = 0.0544
R indexes	R1 = 0.0266	R1 = 0.1243	R1 = 0.0605
(all data)	wR2 = 0.0638	wR2 = 0.1418	wR2 = 0.0596

[a] $R1 = \sum||F_o| - |F_c||/\sum |F_o|$. [c] $wR2 = [\sum w(F_o^2 - F_c^2)^2/\sum w(F_o^2)^2]^{1/2}$.

Two different commercially available supports were used: muscovite mica and highly oriented pyrolitic graphite (HOPG). Both were cleaved with adhesive tape.

Sample preparation for AFM. Procedure A. One milligram of crystals of compound **4** was treated with 1 mL of NaOH (0.1 mol L^{-1}). The resulting solution was centrifuged at 40 000 rpm for 10 min, and a drop of the clear solution was deposited on a cleaved mica sheet previously treated with aminopropyltriethoxysilane. The drop was left in contact with the mica for 10 min and then washed with milliQ water.

Procedure B. Ten microliters of a water solution of $Cd(ClO_4)_2 \cdot 6H_2O$ (10^{-9} mol L^{-1}) was mixed with 20 μL of a water solution of 6-MP (10^{-9} mol L^{-1}); 20 μL of the resulting solution was immediately deposited on recently cleaved HOPG. The sample was then left in air to allow complete evaporation of the drop, and then it was heated at 80 °C for 1 h.

Physical Measurements. ^{1}H NMR measurements (300 MHz) were carried out at room temperature on a Bruker AMX-300 instrument. Chemical shifts are given in parts per million relative to internal tetramethylsylane using deuterated dimethyl sulfoxide (DMSO-d_6) as solvent. The solid-state NMR measurements were determined at room temperature on a Bruker AV 400 WB instrument using cross polarization and magic-angle spinning (CP/MAS) with ∼20 mg samples packed in a 2.5 mm zirconia rotor. Experiments were performed at spinning frequency of 10 kHz. The ^{113}Cd CP/MAS spectra were acquired with a spectral window of 100 kHz using a $\pi/2$ pulse width of 2.5 μs, a 7 ms contact time, and 5 s relaxation delay. FTIR spectra (KBr pellets) were recorded on a Perkin-Elmer 1650 spectrophotometer. Elemental analyses were performed on a Perkin-Elmer 240-B microanalyzer.

X-ray Data Collection and Structure Determination. Data collections on single crystals of compound **1** were carried out at a Bruker-Nonius Kappa CCD2000/Bruker SMART CCD-based diffractometer at 100 K, whereas those of compounds **2** and **3** were measured on an Xcalibur diffractometer at 293 K. Both diffractometers were equipped with an area detector, using graphite-monochromated Cu Kα radiation ($\lambda = 1.54178$ Å) on the Bruker-Nonius Kappa CCD2000 diffractometer and graphite-monochromated Mo Kα radiation ($\lambda = 0.71069$ Å) on the Xcalibur diffractometer. Data were corrected for Lorentz and polarization effects. The structures were solved by direct methods using the SIR 97 program.[12] Full matrix least squares refinements were performed on F^2 using SHELXL97.[13] All non-hydrogen atoms, except those of the nitrate counterions and the crystallization water molecule in compound **2**, were refined anisotropically. This is the result of the poor quality of the crystals of compound **2**. All calculations were performed using the WinGX crystallographic software package.[14] The final geometrical calculations and the graphical manipulations were carried out with the PARST95[15] and PLATON[16] programs. Summaries of crystal data collection and refinement parameters are given in Table 1. Selected bond lengths and angles are listed in Table 2.

AFM Measurements. AFM images were acquired in dynamic mode using a Nanotec Electronica system (www.nanotec.es). Olympus cantilevers were used with a nominal force constant of 0.75 N/m.

Computational Methods. Our calculations were based on density functional theory[15] (DFT) as implemented in the SIESTA code,[16,17] within the spin-polarized generalized gradient approximation (GGA),[17] with core electrons represented by separable[18] norm-conserving pseudopotentials,[19] including partial core correction for Cd. Several convergence tests (such as structural and magnetic properties of several experimentally known molecules and polymers containing the building blocks of the systems in our study) were

(12) Altomare, A.; Burla, M. C.; Camalli, M.; Cascarano, G. L.; Giacovazzo, C.; Guagliardi, A.; Moliterni, A. G. G.; Polidori, G.; Spagna, R. *J. Appl. Crystallogr.* **1999**, *32*, 115−119.
(13) Sheldrick, G. M. *SHELXS97* and *SHELXL97*; University of Göttingen: Göttingen, Germany, 1997.
(14) Farrugia, L. J. *WINGX. A Windows program for crystal structure analysis*; University of Glasgow: Glasgow, U.K., 1998.
(15) Nardelli, M. *J. Appl. Crystallogr.* **1995**, *28*, 659−673.
(16) Spek, A. L. *PLATON, A multipurpose crystallographic tool*; Utrecht University: Utrecht, The Netherlands, **1998**.
(17) Perdew, J. P.; Burke, K.; Ernzerhof, M. *Phys. Rev. Lett.* **1996**, *77*, 3865−3868.
(18) Kleinman, L.; Bylander, D. M. *Phys. Rev. Lett.* **1982**, *48*, 1425−1428.
(19) Troullier, N.; Martins, J. L. *Phys. Rev. B* **1991**, *43*, 1993−2006.

Table 2. Selected Bond Lengths (Å) and Angles (deg)[a]

		compound **1**	
Cd−S6A	2.740(1)	Cd−N7B	2.333(2)
Cd−N7A	2.319(2)	Cd−S6B	2.637(1)
Cd−O2	2.776(2)	Cd−O1	2.435(2)
Cd−S6A^{i}	2.998(1)		
S6A−Cd−S6A^{i}	82.85(2)	S6B−Cd−O1	99.34(5)
S6A−Cd−N7A	79.90(5)	N7A−Cd−O1	84.69(7)
S6A−Cd−N7B^{i}	83.75(6)	N7B−Cd−O2	122.59(7)
S6A−Cd−O2	71.62(5)	S6A−Cd−S6B^{i}	95.38(2)
S6B−Cd−N7B	81.67(5)	S6A−Cd−N7A^{i}	84.01(6)
N7A−Cd−N7B	106.86(7)	S6A−Cd−O^{i}	153.13(5)
N7B−Cd−O1	76.35(7)	S6B−Cd−N7A	171.29(6)
S6A−Cd−S6B	91.40(2)	S6B−Cd−O2	92.89(5)
S6A−Cd−N7B	164.26(6)	N7A−Cd−O2	84.04(7)
S6A−Cd−O1	118.91(5)	O1−Cd−O2	48.06(6)
S6A−Cd−O2^{i}	153.33(5)		
		compound **2**	
Cd−S6A	2.763(2)	Cd−N7B	2.339(6)
Cd−N7A	2.287(6)	Cd−S6B	2.653(2)
Cd−S6A^{ii}	2.914(2)	Cd−O1w	2.438(6)
S6A−Cd1−S6A^{ii}	84.62(7)	S6B−Cd1−N7B	81.6(2)
S6A−Cd1−N7A	80.2(2)	N7A−Cd1−O1W	88.5(2)
S6A−Cd1−N7B^{ii}	97.6(2)	S6A−Cd1−S6B^{ii}	93.55(7)
S6B−Cd1−N7A	102.0(2)	S6A−Cd1−N7B	96.3(2)
N7A−Cd1−N7B	175.5(2)	S6A−Cd1−O1W^{ii}	169.4(1)
S6A−Cd1−S6B	177.05(8)	S6B−Cd1−O1W	96.0(1)
S6A−Cd1−N7A^{ii}	84.9(2)	N7B−Cd1−O1W	88.5(2)
S6A−Cd1−O1W	86.1(1)		
		compound **3**	
Cd1−N7	2.266(2)	Cd1−S6^{iii}	2.888(1)
Cd1−S6	2.741(1)		
N7−Cd1−N7^{iv}	180.0	N7−Cd1−S6^{iii}	92.33(5)
S6−Cd1−S6^{iv}	180.0	S6−Cd1−S6^{v}	94.65(2)
S6−Cd1−S6^{iii}	85.35(2)	N7−Cd1−S6	80.04(5)
N7−Cd1−S6^{iv}	99.96(5)	N7^{iv}−Cd1−S6^{iii}	87.67(5)

[a] Symmetry code: (i) $-x+1, -y+1, -z$; (ii) $-x, -y+2, -z+1$; (iii) $-x+1, y, -z+1/2$; (iv) $-x+1, -y+1, -z+1$; (v) $x, -y+1, z+1/2$.

performed to ensure that the standard double-ζ basis set, with polarization orbitals (DZP), provided a good description of the systems in the present work. Our study addresses both infinitely long polymer chains and finite molecules (monomers). These were simulated using periodic boundary conditions (PBC) in a supercell, which included large vacuum regions in the two directions perpendicular to the chains for the case of polymers and in all three directions for the monomers to minimize the interaction between periodic images that are present in our calculations resulting from the use of PBC. Our supercell dimensions were chosen to ensure that atoms in neighboring molecules were at least 9 Å apart. All the geometries were optimized, with residual forces on each atom of less than 0.04 eV/Å. This methodology[20,21] has been successfully applied to many different biomolecular systems in previous studies.[22,23]

Results and Discussion

One-dimensional materials have been described as one of the most useful systems for technological applications.[1] In recent years, supramolecular coordination chemistry has produced a large number of 1D coordination polymers with interesting potential applications. In principle, the use of nucleobases as building blocks for the construction of 1D coordination polymers may yield structures resembling DNA.[11,24,25] 6-Mercaptopurine is a synthetic purine nucleobase which is the thio analogue to the natural hypoxanthine. Its coordination chemistry has been well established[26] in part because this ligand presents itself as a clinical agent for the treatment of human leukemia. Despite the versatility in its coordination modes, only a few X-ray structures have been described, most of them of monomeric complexes with just a few being dimeric or polymeric complexes.[26]

Scheme 1 provides a representation of the routes employed for the synthesis of the different Cd(II) complexes with 6-mercaptopurine (6-MP). The direct reaction between 6-MP and $Cd(NO_3)_2$, in methanol, leads to formation of the dimer complex **1**. Figure 1 provides a view of the X-ray structure obtained for compound **1**. The molecular cation of compound **1** consists of a cadmium dimer complex in which two different types of 6-MP ligands are present: (i) one acting as a terminal chelate ligand binding to the Cd(II) through N(7) and S(6) and (ii) another acting as a bridging ligand coordinating to the metal cations through the S(6) and forming a chelate with the N(7) atom. The Cd(II) cations are seven-coordinate with irregular coordination geometry. It can be described as an equatorial plane formed by the two chelating 6-MP ligands with the remaining apical positions being filled by two asymmetrically coordinated oxygen atoms ($\Delta d = 0.34$ Å) of a nitrate anion in the upper side and a sulfur atom from a 6-MP ligand chelated to the lower metal atom. The metal atom deviates 0.1603(2) Å from the equatorial plane toward the nitrate anion. The coordination distances and angles within the equatorial plane are similar to those reported for other Cd complexes chelated by 6-MP ligands.[11,27] The sulfur atom of the bridging 6-MP ligand establishes two different Cd−S bond distances: 2.740(1) Å with the chelated metal atom and 2.998(1) Å with the upper cadmium. The 6-MP terminal and bridging ligands are almost collinear (dihedral angle = 6.69(5)°), but the coordinate nitrate anions are significantly deviated from the plane defined by the two Cd and the sulfur atoms of the bridging ligands (the two oxygen atoms of the nitrate deviate 0.358(3) and 0.613(2) Å, respectively). It should be noted that the terminal and bridged 6-MP ligands present the N(7) atoms in a cis disposition. The coordination sphere of the Cd(II) is completed by a nitrate ion which is bound to the metal as a chelate. The three-dimensional cohesiveness of the crystal structure is achieved by means of electrostatic interactions between the nitrate counterions and the cationic dimeric entities and an extensive network of hydrogen bonds (Figure 1). The bridging 6-MP ligands establish double centrosymmetric N(9)−H···N(3) hydrogen bonds (N(9A)···N(3A) =

(20) Ordejon, P.; Artacho, E.; Soler, J. M. *Phys. Rev. B* **1996**, *53*, 10441−10444.
(21) Soler, J. M.; Artacho, E.; Gale, J. D.; Garcia, A.; Junquera, J.; Ordejon, P.; Sanchez-Portal, D. *J. Phys. Cond. Mater.* **2002**, *14*, 2745−2779.
(22) de Pablo, P. J.; Moreno-Herrero, F.; Colchero, J.; Herrero, J. G.; Herrero, P.; Baro, A. M.; Ordejon, P.; Soler, J. M.; Artacho, E. *Phys. Rev. Lett.* **2000**, *85*, 4992−4995.
(23) Alexandre, S. S.; Artacho, E.; Soler, J. M.; Chacham, H. *Phys. Rev. Lett.* **2003**, *91*, 108105.
(24) Shipman, M. A.; Price, C.; Elsegood, M. R. J.; Clegg, W.; Houlton, A. *Angew. Chem., Int. Ed.* **2000**, *39*, 2360−2362.
(25) Fusch, E. C.; Lippert, B. *J. Am. Chem. Soc.* **1994**, *116*, 7204−7209.
(26) Dubler, E. In *Metal Ions in Biological Systems*; Sigel, A, Sigel, S., Eds.; Marcel Dekker: New York, 1996; Vol. 32, pp 301−338.
(27) Griffith, E. A. H.; Amma, E. L. *Chem. Commun.* **1979**, 1013−1014.

Scheme 1. Schematic Representation of the Routes Employed in the Syntheses

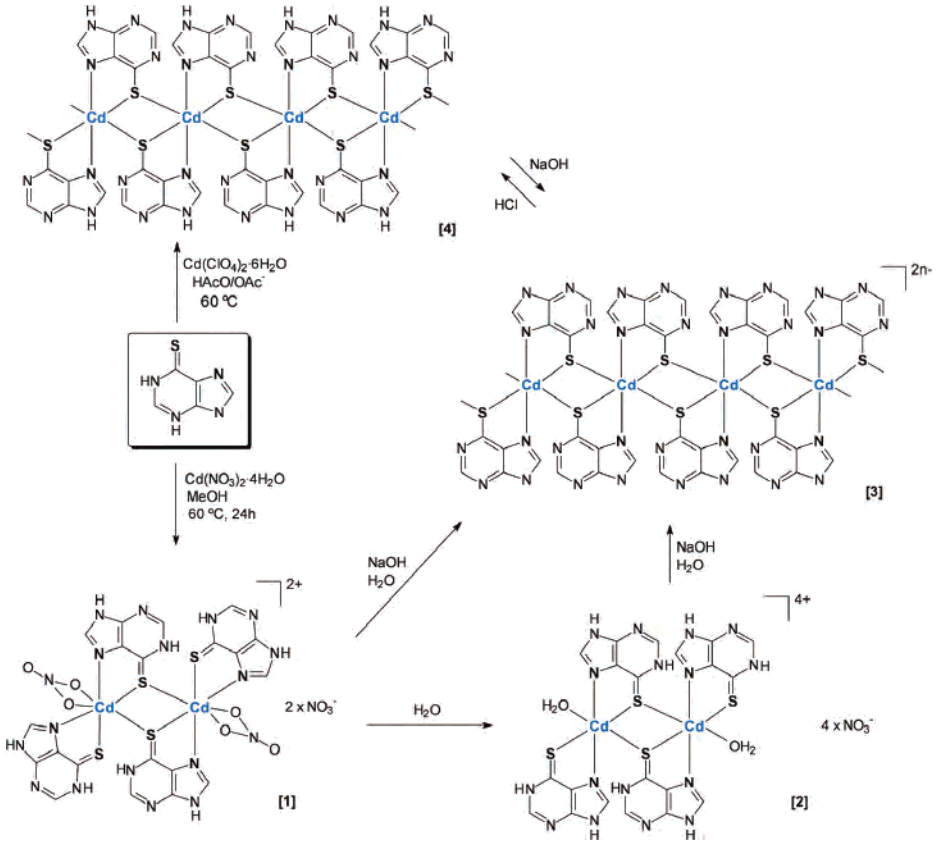

3.043(3) Å) that generate supramolecular ladderlike chains of dimer entities that run along the [110] direction for dimers placed at $z = 0$ or 1 and along the [1−10] direction for those placed at $z = 1/2$. There is no evidence of direct interaction between chains placed at the same z level, but ladders of different levels are linked together through a hydrogen bond between the donor N9B−H group and the acceptor O1 atom (N(9B)···O(1) = 2.834(3) Å) belonging to a nitrato ligand of a dimer from the adjacent layer. The remaining N1A and N1B donor atoms of the mercaptopurine ligands are used to fix the nitrate counterions.

When compound **1** is stirred in water (pH 7), partial hydrolysis takes place by substitution of the coordinated nitrate by water molecules affording a new dimer complex **2**. The crystal structure of compound **2** is closely related to that of **1**, in both cases the complex entity consists of cadmium dimers where the metal centers are bridged by two symmetry center related μ-6-MP-*S(6),N(7):S(6)* ligands. The sphere of coordination is completed by a terminal chelating 6-MP and a water molecule leading to an octahedrical coordination environment for the metal centers. This octahedral environment can be described as an equatorial plane formed by the S(6) and N(7) atoms of the chelating terminal and bridging ligands and the apical positions being occupied by the S(6) atom of the bridging 6-MP coordinated to the other metal center and by a water molecule that replaces the coordinated nitrate ion of compound **1**. Another substantial difference between both structures is the relative disposition of the terminal and bridging 6-MP ligands in a cis arrangement for compound **1** and a trans one for compound **2**. The different arrangements imply a very interesting issue about the transformation process from compound **1** to **2**, this indicates that it is not only a simple replacement of a nitrate anion by a water molecule but also involves a rearrangement of the terminal 6-MP ligand around the cadmium. A plausible mechanism for this transformation has been proposed in Figure S1. The crystal structure also includes crystallization water molecules and nitrate counterions which occupy the voids generated in the crystal packing of the complex entities (Figure 2). The dimeric entities are held together by means of symmetry center-related double hydrogen bonds between the N(1) atom of the bridging 6-MP ligand and a water molecule coordinated to the adjacent dinuclear unit, leading to hydrogen-bonded chains of dimers spreading out parallel to the *a* axis. These chains are surrounded by crystallization water molecules and nitrate counteranions, which are responsible for the cohesiveness of the crystal packing because they join the chains together through an extensive hydrogen-bond network. Weak interactions between the 6-mercaptopurine ligands have been observed through a bifurcated C(2)−H hydrogen bond established with nitrate counteranion and the N(3) atom of the adjacent dimeric entity (Figure S2). A special feature of this supramolecular network is the presence of hydrogen bonded hexagons formed by four water molecules and two nitrate anions (Figure 2c).

The deprotonation of the N(1) and N(9) positions of the 6-MP ligands in compound **2** allows self-assembly of the generated dimetallic subunits between them to give the coordination polymer **3**. This can be achieved by the addition of NaOH to a suspension of either complex **1** or **2** (reaching

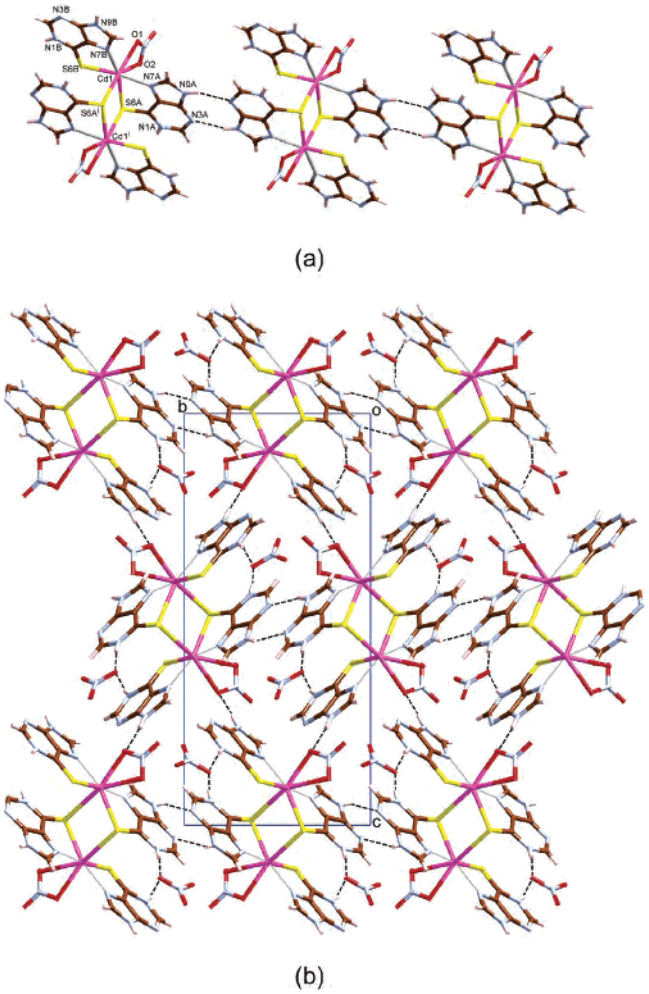

Figure 1. One-dimensional arrangement of the dinuclear units in compound **1** (a). A view of the crystal packing along [100] direction. Dashed lines represent the hydrogen-bonding scheme (b).

up to pH 12). From several metal cations tested to obtain suitable monocrystals for a X-ray study, it was only possible with Ca(II). Interestingly, in compound **3** the new 1D coordination polymer formed is a polyanion which neutralizes its charge in the solid state with a polycation formed by $[Ca(OH_2)_6]_n^{2n+}$.

The structure of compound **3** consists of parallel anionic chains of $[Cd(6\text{-}MP^{2-})_2]_n^{2n-}$ and cationic chains of $[Ca(H_2O)_6]_n^{2n+}$ which are joined together by means of electrostatic interactions and hydrogen bonds. The one-dimensional anionic complex is based on stacked centrosymmetric $[Cd(6\text{-}MP^{2-})_2]$ entities, which are linked one to each other through Cd−S bonds, forming a one-dimensional chain along the crystallographic *c* axis. The coordination mode of the doubly deprotonated mercaptopurine ligand is similar to that reported for the bridging ligands in compounds **1** and **2**. The ligand chelates the metal center through the N(7) and S(6) atoms and binds the cadmium atom from the upper entity through the S(6) atom. The metal atom is slightly displaced from the mean plane of the mercaptopurine ligand (0.011(2) Å). The distance between metal centers of consecutive entities is 4.139(1) Å, but the stacking of the planar entities is not perfectly parallel; the dihedral angle between consecutive entities is 5.11(6)°. It is worth noting that in the related crystal structure of the one-dimensional $[Cd(6\text{-}MP^{-})_2]_n$ polymer reported by Dubler and Gyr[11] (compound **4** in Scheme 2), the chain can also be described as the packing of centrosymmetric $[Cd(6\text{-}MP^{-})_2]$ entities through axial Cd−S bonds. However, the packing between adjacent entities is parallel and the M···M distance within the chain is 3.918 Å. An interesting issue is the different shape of the two polymeric chains and the prevalence of the trans disposition in the [Cd(6-MP$^-$)2] entities. Scheme 2 shows the four possible types of polymeric chains that can be achieved. It is interesting that only the trans disposition allows the generation of linear chains, whereas the cis disposition leads to either *zigzag* or helical chains which are more difficult to assemble together. The main difference between the two linear chains is the establishment of intramolecular $\pi-\pi$ interactions between adjacent 6-MP ligands which are the most favorable in compound **4** because the arrangement of the chain allows every mercaptopurinate ligand to establish $\pi-\pi$ interactions with the two adjacent ligands. In compound **3**, the presence of these interactions is hampered by the repulsive electrostatic force between the doubly deprotonated mercaptopurines, which leads to a chain arrangement that minimizes it. In this case, the chain only allows the presence of $\pi-\pi$ stacking with just one of the two adjacent mercaptopurinate ligands, and even this stacking is weakened by a nonparallel divergent disposition (5.11(6)°, Figure S3). Another effect of the increased negative charge is the elongation of the M···M distance (4.139(1) vs 3.918(3) Å in compound **4**).

The cationic aquo−metal chain structure that provides electrical neutrality to the overall structure is based on distorted square antiprisms sharing opposite edges. Chains of aquo−metal complexes of s-block cations are unusual. To our knowledge, there are only examples of one-dimensional aquo-metal complexes with sodium cations[28−35] reported, and the only reported aquo-calcium polynuclear complex is a dimeric entity formed by two square antiprisms sharing an edge.[28] The three-dimensional overall structure is achieved by the simple assembly of anionic and cationic chains as can be observed in Figure 3.

Finally, the presence of bridging neutral, monoanionic, and dianionic 6-mercaptopurine ligands with the same coordination mode give us a deeper insight into the chemical and structural implications of the deprotonation. First of all, with respect to the thione/thiol tautomerism, our crystallographic data support the thione tautomers in compounds **1** and **2**.

(28) Freisinger, E.; Lippert, B. *J. Inorg. Biochem.* **2001**, *86*, 222−222.
(29) Sagatys, D. S.; Dahlgren, C.; Smith, G.; Bott, R. C.; White, J. M. *Dalton Trans.* **2000**, 3404−3410.
(30) Biesemeier, F.; Harms, K.; Muller, U. *Z. Kristallogr.—New Cryst. Struct.* **2004**, *219*, 39−40.
(31) Kennedy, A. R.; Kirkhouse, J. B. A.; McCarney, K. M.; Puissegur, O.; Smith, W. E.; Staunton, E.; Teat, S. J.; Cherryman, J. C.; James, R. *Chem.—Eur. J.* **2004**, *10*, 4606−4615.
(32) Huang, W.; Xie, X. K.; Cui, K.; Gou, S. H.; Li, Y. Z. *Inorg. Chim. Acta* **2005**, *358*, 875−884.
(33) Nathan, L. C.; Mai, T. D. *J. Chem. Crystallogr.* **2000**, *30*, 509−518.
(34) Ma, C. B.; Chen, C. N.; Chen, F.; Zhang, X. F.; Zhu, H. P.; Liu, Q. T.; Liao, D. Z.; Li, L. C. *Bull. Chem. Soc. Jpn.* **2003**, *76*, 301−308.
(35) Kashiwagi, T.; Sano, C.; Kawakita, T.; Nagashima, N. *Acta Crystallogr. C* **1995**, *51*, 1053−1056.

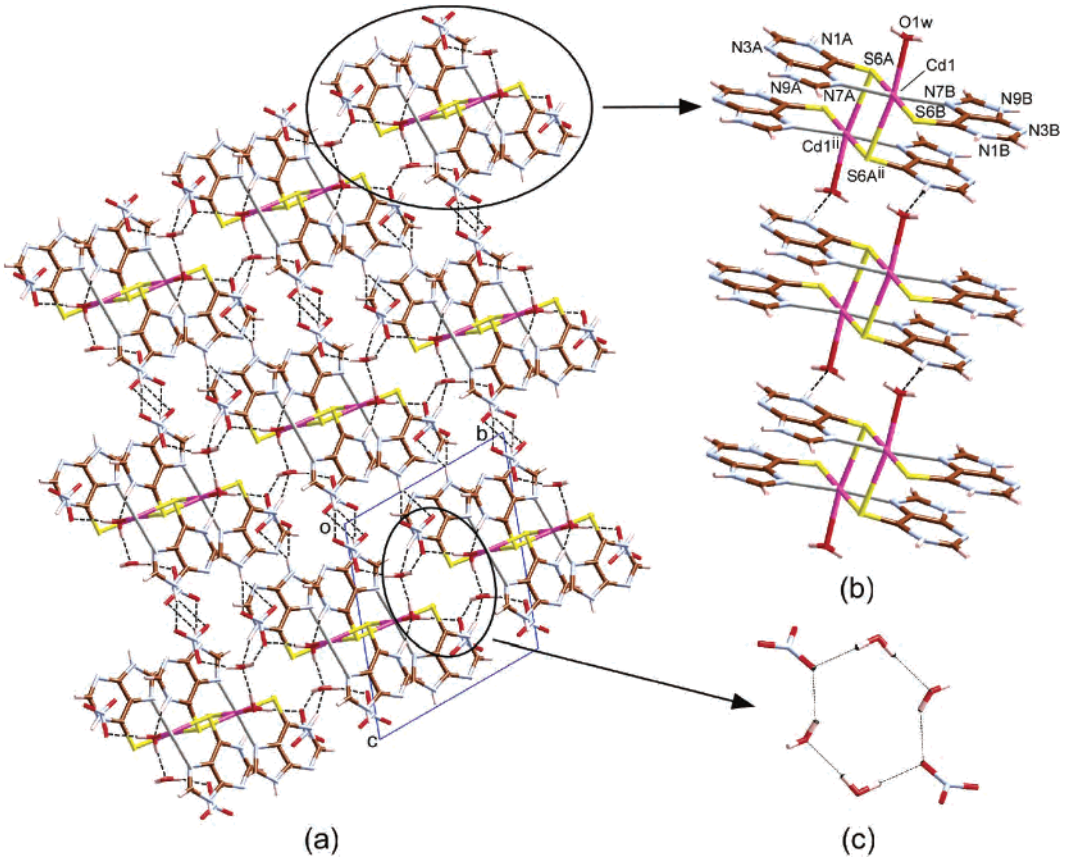

Figure 2. A view of the crystal packing (a) along [100] direction of compound **2**, showing the one-dimensional arrangement of the dimeric entities (b) and the hydrogen bonded hexagons formed by four water molecules and two nitrate anions (c). Dashed lines represent the hydrogen-bonding scheme.

The major effect of the deprotonation of a ring nitrogen atom in the purine derivatives is the narrowing of the corresponding C−N−C angle by about 3−4°.[26] The compounds reported herein are good examples of this: the values of these angles in compounds **1** and **2** (*1H,9H*-6-MP) are 123.8(2) and 124.7(7)° around N(1) and 107.5(2) and 107.2(6)° around N(9), whereas in compound **3** (6-MP^{2-}), the values of the angles show the expected decrease: 117.8(2)° for N(1) and 102.6(2)° for N(9). However in compound **4**, the C−N−C bond angles (120.2(3) and 105.2(4)° for N(1) and N(9), respectively) are exactly between the ones given for the compounds **1**−**3** of neutral and double deprotonated mercaptopurine ligands. This fact seems to indicate that in compound **4**, the hydrogen atom is disordered over the N(1) and N(9) atom with half occupation factors (*1H*-6-MP^{-}/*9H*-6-MP^{-}), instead of being fully placed on N(9) (*9H*-6-MP^{-}) as reported by Dubler and Gyr.[11] Another way to confirm this hypothesis is based on the crystal structure; the analysis of the interactions among almost coplanar 6-mercaptopurine ligands shows two usual hydrogen bond distances of 2.755(5) Å for N(9)···N(9) (with two hydrogen atoms placed between them) and 2.806(5) Å for N(1)···N(1) (without any hydrogen atom between them). These hydrogen bonds are only possible if we assume the presence of both *1H*-6-MP^{-} and *9H*-6-MP^{-} tautomers within the structure (Figure S4), as is also suggested by the values of the angles around N(1) and N(9). On the other hand, the thione form of the neutral 6-MP ligand in compounds **1** and **2** is confirmed by the analysis of the corresponding C−S bond distances, which are in the range of 1.66−1.70 Å, and also by the location of the hydrogen atom at its usual N(1) position. The change in this structural parameter with the deprotonation indicates a small but significant trend toward lengthening of the C(6)−S(6) bond length and therefore toward more single-bond character: 1.703(3) for **1**, 1.702(7) for **2**, 1.724(3) for **4**, and 1.745(2) Å for **3**. The intramolecular distance between S(6) and N(7) (called as "bite" distance of the ligand) is a typical feature for the 6-mercaptopurines reflecting the binding mode of these ligands.[26] In the free ligand, the bite distance is 3.35 Å, while when chelation occurs, the bite distance is decreased as a function of the ionic radius of the metal. The bite distances found for Cd(II) complexes are typically 3.24−3.32 Å. Therefore, the bite distances of 3.265(2) and 3.272(7) Å for the dinuclear compounds **1** and **2** and 3.240(2) Å for the polymer **3** (same for **4**) fall in the expected range and do not seem to be affected by the deprotonation of the ligand.

As mentioned above, the structures found by X-ray diffraction for the polyanionic chain **3** (structure A) and the polymer **4** (structure B) show small differences (Scheme 2). This suggests the possibility that each of the polymers could present not only the structure found by the X-ray studies but both structures, A and B. To address this possibility, DFT calculations have been performed for the polyanion of **3** and the polymer **4** in structures A and B.

The first set of calculations was performed to check the stability of both compounds against the isolated monomers

Scheme 2. Plausible Types of Polymeric Chains

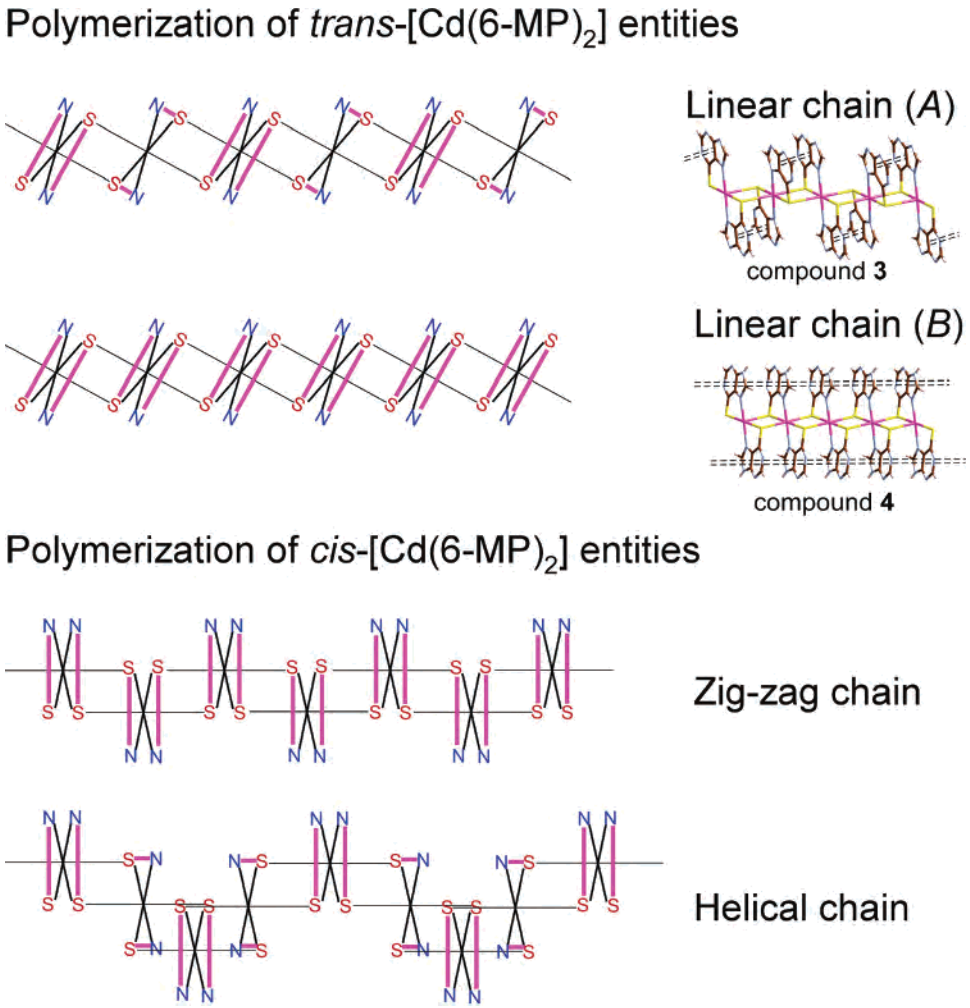

in both structures. We found a binding energy of 0.38 eV/bond for the polyanion of **3** in structure A, with a metal−metal distance of 4.19 Å for the structure corresponding to the energy minimum. However, the monomer is more stable than structure B for this compound, indicating that this latter structure is not stable for the polyanion of **3** (**3** in the B form does not converge to a polymeric stable structure). These results are in agreement with the experimental structure and

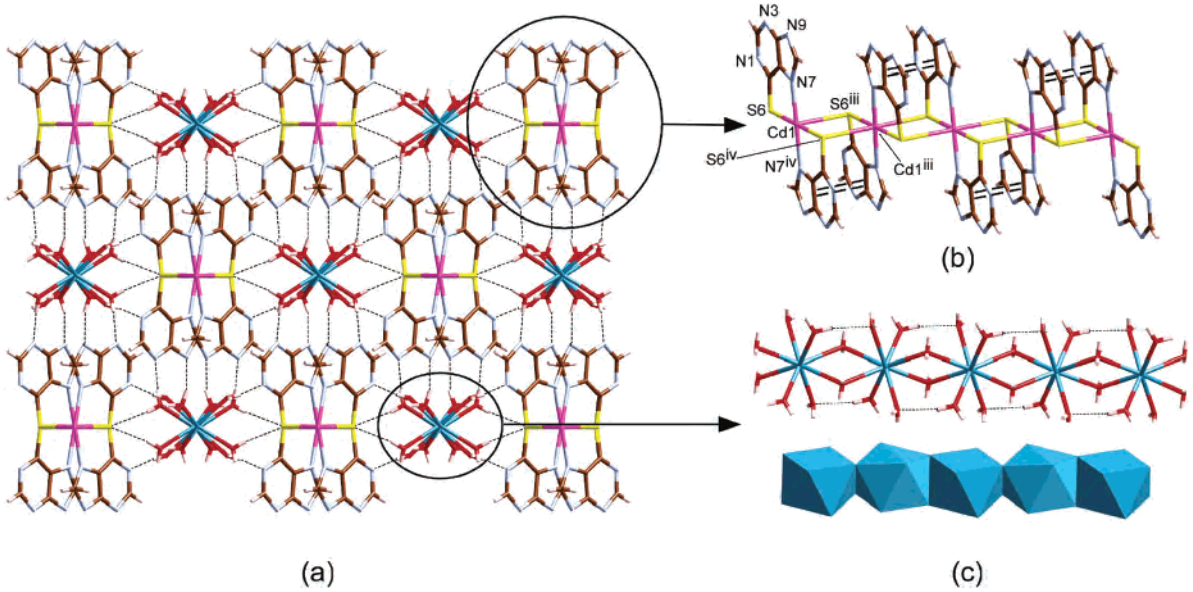

Figure 3. A view of the crystal packing (a) along [001] direction of compound **3**, showing the one-dimensional $[Cd(6\text{-}MP^{2-})_2]_n^{2n-}$ anionic chains (b) and the one-dimensional $[Ca(H_2O)_6]_n^{2n+}$ anionic chains (c). Dashed and double-dashed lines represent hydrogen bonds and $\pi-\pi$ interactions, respectively.

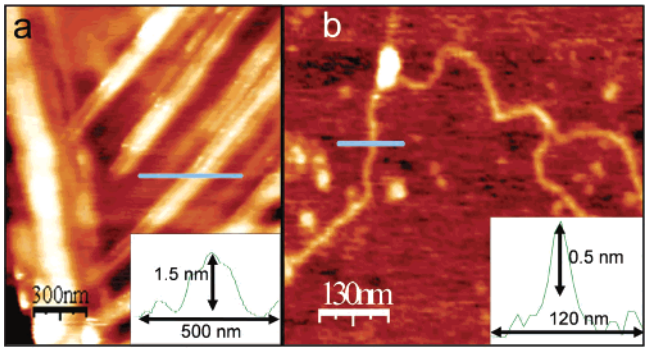

Figure 4. (a) AFM topographic image of the crystals obtained by treating **4** with NaOH (without centrifugation). (b) AFM topographic image of a single polyanion obtained by the method described in the Experimental Section (sample preparations for AFM, procedure A).

can be explained by the repulsive electrostatic forces established between the doubly deprotonated mercaptopurine ligands, as mentioned above.

For polymer **4**, structures A and B are stable with Cd−Cd distances of 4.09 and 3.92 Å, respectively. In this case, the compound is stable against the monomer in both structures, with binding energies of 0.48 eV/bond for both structures (A and B), within the error of the calculation (the difference in energy between the two structures is only of 8 meV per formula unit). Therefore, from the theoretical point of view both structures are plausible for the polymer **4**. The efforts to isolate compound **4** with structure A following the synthetic route through the dimers **1** and **2** (Scheme 1) failed, yielding a microcrystalline solid which has an X-ray powder diffraction pattern similar to the one obtained for polymer **4** (structure B) in the direct reaction.

One-dimensional coordination polymers are usually insoluble in most of the solvents or their solubilization leads frequently to decomposition. Recently, we have provided the first example of the isolation and morphological and electrical characterization of single chains of a one-dimensional coordination polymer.[8] In that case, isolated single chains on a treated mica surface are obtained by ultrasonication of crystals of compound **4** in ethanol.

The deprotonation of compound **4** by NaOH leads to a polyanion analogous to that found in compound **3**: this has been verified by IR and CNHS elemental analysis. However, the solid isolated following this procedure is amorphous. Figure 4a shows a nanocrystal obtained by treating crystals of compound **4** with NaOH. This situation can be considered to be an intermediate state of the deprotonation process and disgregation of crystals of compound **4**. One can see fibrous structures going out of a central bigger one. We suggest that this structure is the result of the partial deprotonation of compound **4** crystals by NaOH. Figure 4b shows a linear

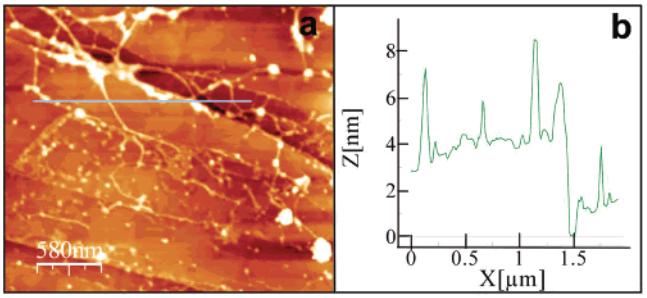

Figure 5. (a) AFM topographic image of the fibers obtained by in situ reaction on HOPG. (b) Topographic profile across the line in (a).

molecule of ∼0.5 nm in height (value in agreement with the X-ray height of a single polymer). This molecule is probably a single polyanion obtained by the complete deprotonation of compound **4**.

Another method employed to obtain isolated fibers and single polymers was the in situ reaction at low concentration (10^{-9} mol L^{-1}) between Cd(II) salt and 6-MP on HOPG (a similar reaction carried out in solution gave compound **4**).[11] Figure 5a shows a spider-network consisting of single polymers and fibers of compound **4** with a height ranging from 0.5 to 5 nm (Figure 5b). Additional images of the in situ reaction are provided in the Supporting Information.

In summary, a detailed study on the reaction pathways between Cd(II) and 6-MP has been carried out, leading to the development of an alternative route to prepare the neutral polymer $[Cd(6\text{-}MP^{-})_2 \cdot 2H_2O]_n$ (**4**) and the ionic polymer $[Cd(6\text{-}MP^{2-})_2]_n[Ca(H_2O)_6]_n$ (**3**), through the formation of the dimeric complexes $[Cd_2(6\text{-}MP)_4(NO_3)_2](NO_3)_2$ (**1**) and $[Cd_2(6\text{-}MP)_4(H_2O)_2](NO_3)_4 \cdot 2H_2O$ (**2**). On the basis of these reactions, two new methods for suitable surface deposition and AFM characterization of the one-dimensional coordination polymers obtained have been described: (i) in situ direct reaction of Cd(II) salt and 6-MP on HOPG and (ii) in situ deprotonation of the 6-MP ligands on mica. The development of alternative strategies to study these types of polymers on surfaces opens the possibility of performing nanoscale studies on their properties and their potential uses as nanomaterials.

Acknowledgment. Dedicated to Prof. Bernhard Lippert on the occasion of his 60th birthday. Financial support from MAT2004-05589-C02-01-02, NAN2004-09183-C10-06, and MAT2005-03047.

Supporting Information Available: X-ray crystallographic files in CIF format, Figures S1−S5, Tables S1−S4, input coordinates and optimized structures calculated for compounds **3** and **4** are given in Table S5, and additional AFM images. This material is available free of charge via the Internet at http://pubs.acs.org.

IC060384F